The Global Land Surface Temperature Change in the 21st Century—A Satellite Remote Sensing Based Assessment

Li Lin, *Member, IEEE*, Liping Di, *Senior Member, IEEE*, Chen Zhang, *Member, IEEE*, and Liying Guo, *Member, IEEE*

***Abstract*—Changes in land surface temperature (LST) affect human society and the natural environment, especially for agricultural activities. In recent decades, satellite remote sensing has been used as an alternative approach to ground observation sites for monitoring LST. Prior research has offered broad insights into global and continental-level LST changes, yet these studies have utilized coarse resolutions and have not delved into the intricate spatial and temporal fluctuations. Simultaneously, recognizing the vital significance of LST changes is essential for advancing climate-smart and sustainable agricultural practices. This study utilizes the MODIS product from 2003 to 2021 on the Google Earth Engine to assess the LST change for the entire Earth's land surface. The study quantified the LST changes for the past 19 years at 1-km spatial resolution. We found that the global mean LST has increased by 0.38 °C from 2003 to 2021, and is mainly concentrated on high latitude regions, potentially boosting agriculture activities in these regions. The result also shows that the urban areas are experiencing a rapid LST increase, at a rate of 18% faster than the global average. The outcomes of this study offer invaluable insights, serving as a crucial compass for informed farming decision-making and climate-smart agro-geoinformation studies.**

***Index Terms*—Climate change, land surface temperature (LST), MODIS.**

I. Introduction

ACCORDING to the Sixth Assessment Report (AR6) of the Intergovernmental Panel on Climate Change (IPCC), the increase in global surface air temperature (SAT) (including land and oceans) is projected to reach or exceed 1.5 °C in the near term compared to 1850–1900 [1]. Past studies for estimating global SAT have been model-based and employed in situ data measured by sparsely distributed weather stations [2], [3], [4]. For instance, Global Historical Climatology Network is one of the most popular meteorological station-based datasets for quantifying global temperature [5], [6], and scientists have developed a few indicators to estimate the average global temperature by incorporating the station data [7], [8], [9]. Although a huge success has been achieved in modeling the SAT using the traditional approach, it cannot accurately model and measure the land surface temperature (LST) since the temporal variation of LST is significantly greater than SAT [10].

The temporal change of the Earth's LST is a key indicator of climate change and affects human society and the natural environment [5], [10], [11], [12], [13], [14], [15], [16]. For instance, LST is one of the most important parameters in the farming decision-making process during the growing seasons. The continuous monitoring of fine-resolution LST change at the global level is impossible without the support of satellite remote sensing [10]. The estimation of LST from satellite sensors has improved significantly in past years as many algorithms have been developed and refined [10]. Landsat missions provide thermal data using long-wave infrared (LWIR) bands, with a 30-m spatial resolution and a 16-day temporal resolution. In contrast, MODerate Resolution Imaging Spectroradiometer (MODIS) can measure global LST much more frequently (twice a day) using two LWIR bands. Although the spatial resolution of MODIS is not as fine as Landsat, the 1-km spatial resolution is ideal for measuring LST change at the global scale and has been adopted in many studies [17], [18], [19], [20], [21], [22]. Past study has used multiple coarse-resolution MODIS data (6 km to 1°) to calculate the daily mean surface temperatures [20]. However, the accuracy of the measurement is impacted by cloud coverage (areas with frequent cloud cover will have less accurate measurements). In addition, the surface temperature function used in the previous study was a good model for daily temperature estimation, but not ideal for multiyear or diurnal analysis since it lacks an explanation of temporal variation [20]. Some other studies have also summarized the computational difficulties in measuring large-scale LST changes at high spatial resolution and monitoring both short- and long-term temperature changes [10], [14], [23].

To overcome these problems, we developed a simple and effective method to calculate the MODIS-based LST changes from 2003 to 2021 at a spatial resolution of 1 km for the entire Earth. In this study, both daytime and nighttime LST changes are quantified using linear regression. The study improves the knowledge of the global LST change by 1) explicitly delineating the spatial variation and 2) quantitatively measuring the temporal trends of LST change in different regions to support future LST anomaly studies.

Manuscript received 11 September 2023; revised 5 November 2023 and 21 November 2023; accepted 23 November 2023. Date of publication 4 December 2023; date of current version 22 December 2023. This was supported in part by NASA under Grant 80NSSC20K1262. *(Corresponding author: Liping Di.)*

The authors are with the Center for Spatial Information Science and Systems, George Mason University, Fairfax, VA 22030 USA (e-mail: llin2@gmu.edu; ldi@gmu.edu; czhang11@gmu.edu; lguo2@gmu.edu).

Digital Object Identifier 10.1109/JSTARS.2023.3338980

II. Data and Method

A. Study Area

The study examines the changes in land surface temperature for the entire globe. The spatial extent is −180° to 180° longitudes and −88° to 83° latitudes. Because the exact boundary between continents and oceans can vary by different definitions, the extents of the MODIS daily LST measurements, which are extracted using a land/water mask, are used to determine the boundary of Earth's land surface in this study. The temporal coverage of the LST time series is from January 2003 to December 2021, covering nearly the first two decades of the 21st century.

B. Satellite Data

Both Terra (MOD11A1 V6.1) and Aqua (MOD11A1 V6.1) (and corresponding quality layers) are acquired and processed on the Google Earth Engine (GEE) [24], [25]. GEE is an online geospatial processing platform that provides service with direct access to a large set of global datasets [24]. It provides convenient tools to process a vast amount of satellite data rapidly and accurately [26]. Although Terra satellite started operation in early 2000, data from Aqua were not available until late 2002 [27]. Meanwhile, the selection of annual minimum, mean, median, and maximum requires complete observations for the entire calendar year. For these two reasons, only data after 2003 from both satellites are selected in this study. This article uses the refined MODIS LST (Version 6.6), and the accuracy has already been evaluated and validated in many studies [28], [29]. To delineate LST change in the urban area, the study compares the LST changes for the entire globe and in urban extents using a recently published satellite-based global dataset of annual urban extents [30]. The dataset covers global urban extents at 1-km spatial resolution from 1992 to 2020 and is suitable to represent urban extents for estimating the LST changes in cities.

C. Extracting LST Time Series

For each MODIS pixel, the LST time series for all calendar years (from 2003 to 2021) are sorted and stored in Earth Engine ImageCollection separately. ImageCollection is a collection of stacked images that offers a convenient and efficient method for extracting minimum, mean, median, and maximum values. In the end, each MODIS pixel location will have four sets of numbers indicating the historical minimum, mean, median, and maximum LSTs for 19 years (2003–2021). All LST measurements were then converted into Celsius (°C) from Kelvin (K) for easier interpretation and comparison with other studies.

Oceans in the MODIS LST products were masked out using the MOD03 Land/Water layer during the production [31]. However, due to the boundary inconsistency in the mask layers, the MODIS LST layers are not aligned with each other perfectly, especially in coastal regions. In addition, there are some areas on the Earth constantly covered by clouds, and MODIS satellites cannot see through the cloud and collect LST at these locations. The MODIS quality control (QC) layers were used to address these two issues in this study. For each daily MODIS LST pixel, the corresponding QC layer was examined to ensure it was a clear-sky observation, and the results were compounded in annual stacks. Fig. 1 shows the spatial distribution of clear MODIS observation frequency in 2021. A threshold was utilized to remove pixel locations with less than 50 observations a year (1 observation per week). Data in each year were checked independently ensuring each pixel location has at least 9 years (half of the total study temporal range) of observations, which is crucial to accurately establish the linear regression model.

D. Modeling LST Trend at Pixel Level

Linear regression is one of the simplest but most efficient approaches to model the relationship between the dependent variable and independent variables [32]. A simple linear regression was used to compute the least squares estimates of a linear function for each pixel's LST time series. The year is the independent variable and LST is the dependent variable. For each LST time series, an estimation of the coefficient is identified by finding the least value for the sum of squared errors. The coefficients can reveal both the direction and magnitude of LST changes and are comparable across different regions while mitigating the influence of interannual climate fluctuations in long-term LST changes. The temporal regression models are custom-built for each individual MODIS pixel to ensure the best fitness for different locations. The method has been employed in multiple case studies, and results have proven the feasibility of portraying the temporal variation of LST from different regions [32]. Specifically, the LST variables, including minimum, mean, and maximum values, serve as robust indicators of urban and rural warming as well as global climate change [32]. Four key LST values in each calendar year are identified and input to the regression for minimizing the impact of seasonal variations while keeping the most important LST variables: minimum, mean, median, and maximum values. The calculations of critical LST parameters are outlined in (1)–(4). The minimum and maximum values can represent the extreme temperature (coldest and hottest) conditions, and mean/median values are used to represent the overall temperature condition for each year, respectively. Fig. 2 is an illustration of the calculation of maximum LST for a sample pixel location.

$$\begin{cases} \text{Minimum, the smallest value present in } D & (1) \\ \text{Mean, } \frac{\sum_{i=}^{n} x_i}{n} & (2) \\ \text{Median, the meddle value in } D & (3) \\ \text{Maximum, the largest value present in } D & (4) \end{cases}$$

where n is the number of values in a dataset (D).

III. Results

A. Global LST Temporal Trend Dataset at 1km Resolution

Measuring LST temporal trend is important for global climate change study as it is an important indicator of climate change and one of the most important parameters for understanding the Earth's ecosystem change [32]. In recent years, many scientists have studied the LST changes at the global scale with various indicators and at coarse spatial resolutions [10], [19], [20].

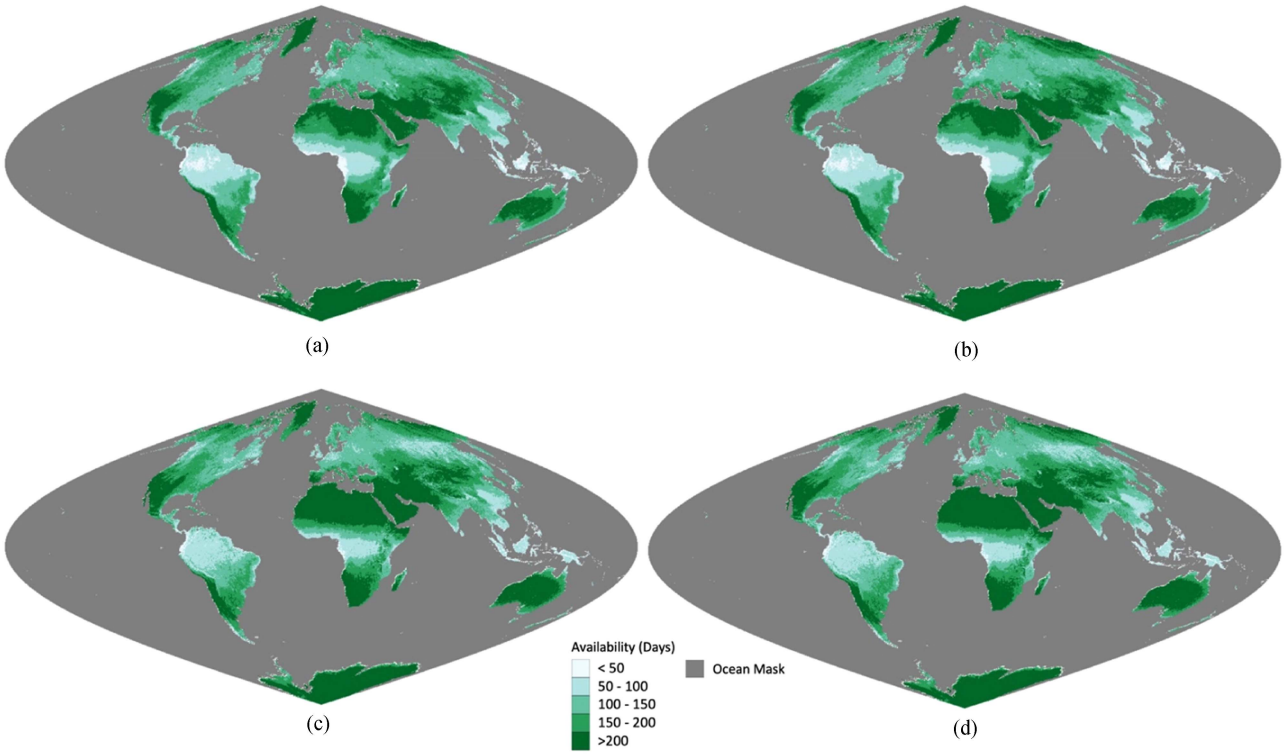

Fig. 1. Annual stack of clear MODIS LST observations for 2021 using MOD11A1/MYD11A1 quality layer. (a) Terra daytime 10:30. (b) Terra nighttime 22:30. (c) Aqua daytime 13:30. (d) Aqua nighttime 1:30. Darker indicates more clear observations, and brighter means fewer clear observations. The highest and lowest possible observations for each location are 366 and 0, respectively. Oceans are masked out and present as light grey.

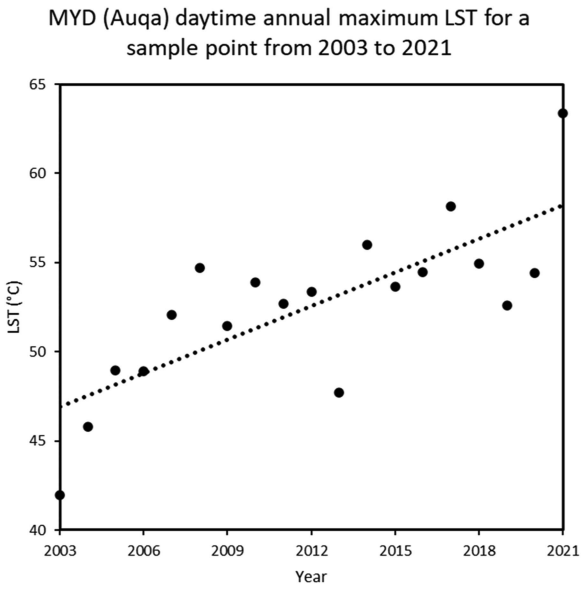

Fig. 2. Regression model for a sample location. Time series of annual daytime maximum LST (Aqua) from 2003 to 2021. The linear regression for the time series is presented as a dotted line. Linear regression models are established for all pixel locations independently.

The variation of global mean temperature has been used most frequently to represent the overall changes for the entire world. However, simply using averaged temperature cannot accurately represent the spatial and temporal variations of the change. For instance, the trends in minimum and maximum LST changes are more important to represent the change in extreme temperatures. Overall LST changes can be delineated using the mean and median LST changes, but the spatial variation is more important and meaningful for scientists and decision-makers. This information is crucial for a better understanding of the spatial and temporal variation of extreme weather for climate studies. Fig. 3 shows the spatial variations of global mean LST changes from 2003 to 2021 using the method proposed in this study. Similar to the mean LST change map, the study also generates maps that delineate the mean, medium, and maximum LST changes for assessment.

B. Assessing Changes in Global LST

Land cover changes such as cropland loss and deforestation can cause dramatic changes in LST. Other factors such as global air warming, changes in atmosphere compositions (e.g., increasing greenhouse gases), air pollution levels, and cloud/fog dynamics also contribute to the change in LST [32]. It is crucial but at the same time very hard to quantify the impacts of these factors on the variation in LST at the global scale since it is impossible to accurately build such a complex model with the injection of all these parameters in fine spatial and temporal resolutions at the global scale. Fortunately, satellite-based LST measurements allow us to examine the spatial and temporal variation of LST at the global scale directly where ground observation sites are scarce. The MODIS Terra and Aqua measure the

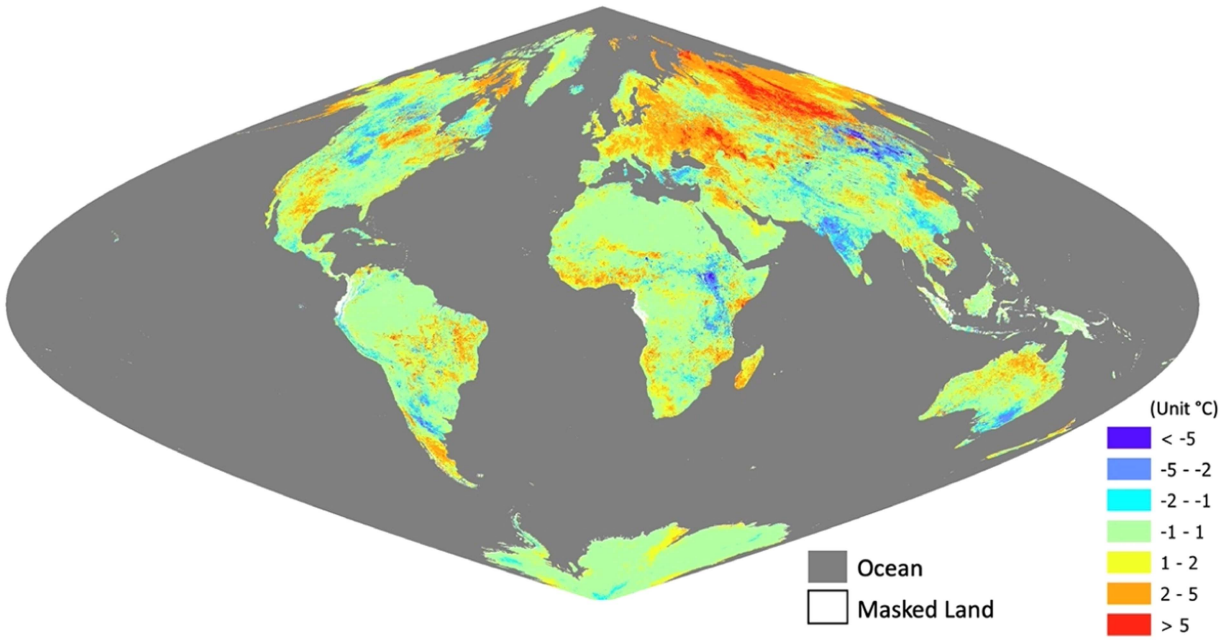

Fig. 3. MODIS-based mean LST changes at 13:30 local time from 2003 to 2021 (unit: °C). Some land areas are masked due to the lack of satellite observations, details are discussed in the method section.

TABLE I
GLOBAL MODIS GLOBAL LAND SURFACE TEMPERATURE (LST) CHANGE RATE BETWEEN 2003 AND 2021 (°C/DECADE)

Satellite	Local time	Minimum	Mean	Median	Maximum
Aqua	1:30	0.29	0.40	0.48	0.28
Terra	10:30	0.01	0.24	0.29	0.25
Aqua	13:30	0.31	0.37	0.44	0.13
Terra	22:30	0.19	0.45	0.57	0.31

Note. Terra MODIS circles a morning orbit and Aqua MODIS an afternoon orbit; numbers in the table measure the LST change in Celsius (°C) per decade.

entire Earth's LST multiple times a day. By combining Terra and Aqua satellite observations together, we are able to extract the 1km spatial resolution LST with very high temporal resolution at the global scale. Table I summarizes the variation of minimum, mean, median, and maximum MODIS LST for the entire globe between 2003 and 2021. The following observations are made from Table I.

1) The overall figures clearly show that all critical LST parameters have increased from 2003 to 2021. In other words, the result suggests a clear pattern of global increase of LST and reconfirms the findings from other studies [1], [6], [19].
2) The nighttime observations (1:30 and 22:30) from different MODIS satellites (Terra and Aqua) have a higher agreement than daytime observations (10:30 and 13:30) which is due to higher temperature variation in the daytime than nighttime.
3) The table also revealed that the average increasing speeds of median LSTs are significantly higher than the minimum, mean, and maximum LSTs, suggesting that it is expected to see more warming days in recent years than 19 years ago.

To better portray the spatial variation of LST temporal trends, it is necessary to assess the LST changes in different regions. Like other studies, this paper calculates the LST changes by latitude groups. Table II highlights the differences in LST changes in the northern and southern hemispheres. The result suggests that the southern hemisphere is experiencing marginal temperature changes compared to the northern hemisphere. In addition, the comparison clearly shows that the temperature changes are more dramatic in the northern hemisphere than in the southern hemisphere. For example, the high increasing speed of minimum LST indicates the warm winters that the northern hemisphere has experienced in recent years.

TABLE II
COMPARISON OF THE MINIMUM, MEAN, MEDIAN, AND MAXIMUM LAND SURFACE TEMPERATURE (LST) CHANGES (°C/DECADE) IN TWO HEMISPHERES AND SEVEN CLIMATE ZONES BETWEEN 2003 TO 2021

Hemisphere / Climate Zone	Time	Minimum	Mean	Median	Maximum
NH (0°– 90°N)	Daytime	0.44	0.46	0.54	0.21
	Nighttime	0.33	0.58	0.73	0.40
SH (0°–90°S)	Daytime	-0.28	0.09	0.12	0.19
	Nighttime	0.11	0.20	0.24	0.14
NH Cold Zone (60°N–90°N)	Daytime	0.20	0.92	1.50	0.25
	Nighttime	0.23	0.96	1.60	0.33
NH Temperate Zone (40°N – 60°N)	Daytime	0.68	0.48	0.29	0.29
	Nighttime	0.45	0.61	0.52	0.46
NH Subtropics Zone (23.5°N – 40°N)	Daytime	0.55	0.05	-0.12	0.19
	Nighttime	0.42	0.27	0.17	0.48
NH Tropical Zone (0°– 23.5°N)	Daytime	0.25	0.09	0.10	-0.02
	Nighttime	0.11	0.24	0.22	0.32
SH Tropical Zone (0°– 23.5°S)	Daytime	0.29	0.26	0.26	0.28
	Nighttime	0.16	0.36	0.39	0.40
SH Subtropics Zone (23.5°S – 40°S)	Daytime	0.30	0.07	-0.08	0.48
	Nighttime	0.19	0.23	0.17	0.27
SH Temperate Zone (40°S – 60°S)	Daytime	0.16	0.65	0.77	0.75
	Nighttime	0.20	0.37	0.44	0.55
SH Cold Zone (60°S – 90°S)	Daytime	-0.65	0.02	0.11	0.06
	Nighttime	0.08	0.14	0.20	0.03

Note. NH: northern hemisphere; SH: southern hemisphere; Daytime LST changes are calculated by averaging Terra MODIS (10:30) and Aqua MODIS (13:30) observations; nighttime LST changes are calculated by averaging Terra MODIS (22:30) and Aqua MODIS (1:30) observations; LSTs in the table measure the changes in Celsius (°C) per decade.

TABLE III
COMPARISON OF THE MINIMUM, MEAN, MEDIAN, AND MAXIMUM LAND SURFACE TEMPERATURE (LST) CHANGES (°C/DECADE) WITHIN URBAN EXTEND BETWEEN 2003 AND 2020 AND THE GLOBAL AVERAGE

Extent	Minimum	Mean	Median	Maximum
Urban*	0.68	0.45	0.27	0.48
Global	0.21	0.38	0.47	0.26

*The urban extent used in this study is calculated from a global annual urban extent dataset [30]. All critical values are calculated using both daytime and nighttime Terra and Aqua observations; LSTs in the table measure the changes in Celsius (°C) per decade.

To clearly show the LST dynamics at different latitude ranges, the LST change data were then aggregated by different climate zones. Climate zones are areas with similar climates and are often classified by latitude (east–west direction around the Earth). Advanced classification methods have been implemented to identify global climate zones for various studies [33]. However, the resolution of these classification results varies and cannot be directly used in deriving the MODIS LST temporal trends in this research. To avoid the complexities, this study adopts the classical method with four major climate zones: Tropical Zone from 0° to 23.5°, Subtropics Zone from 23.5° to 40°, Temperate Zone from 40° to 60°, and Cold Zone from 60° to 90°, for both hemispheres. The LST changes for different climate zones are computed and summarized in the second portion of Table II. The northern hemisphere Cold Zone has the highest increasing speed of LST compared to other climate zones and this phenomenon has been widely observed and proven in many studies. However, the statistics show that not the entire globe is

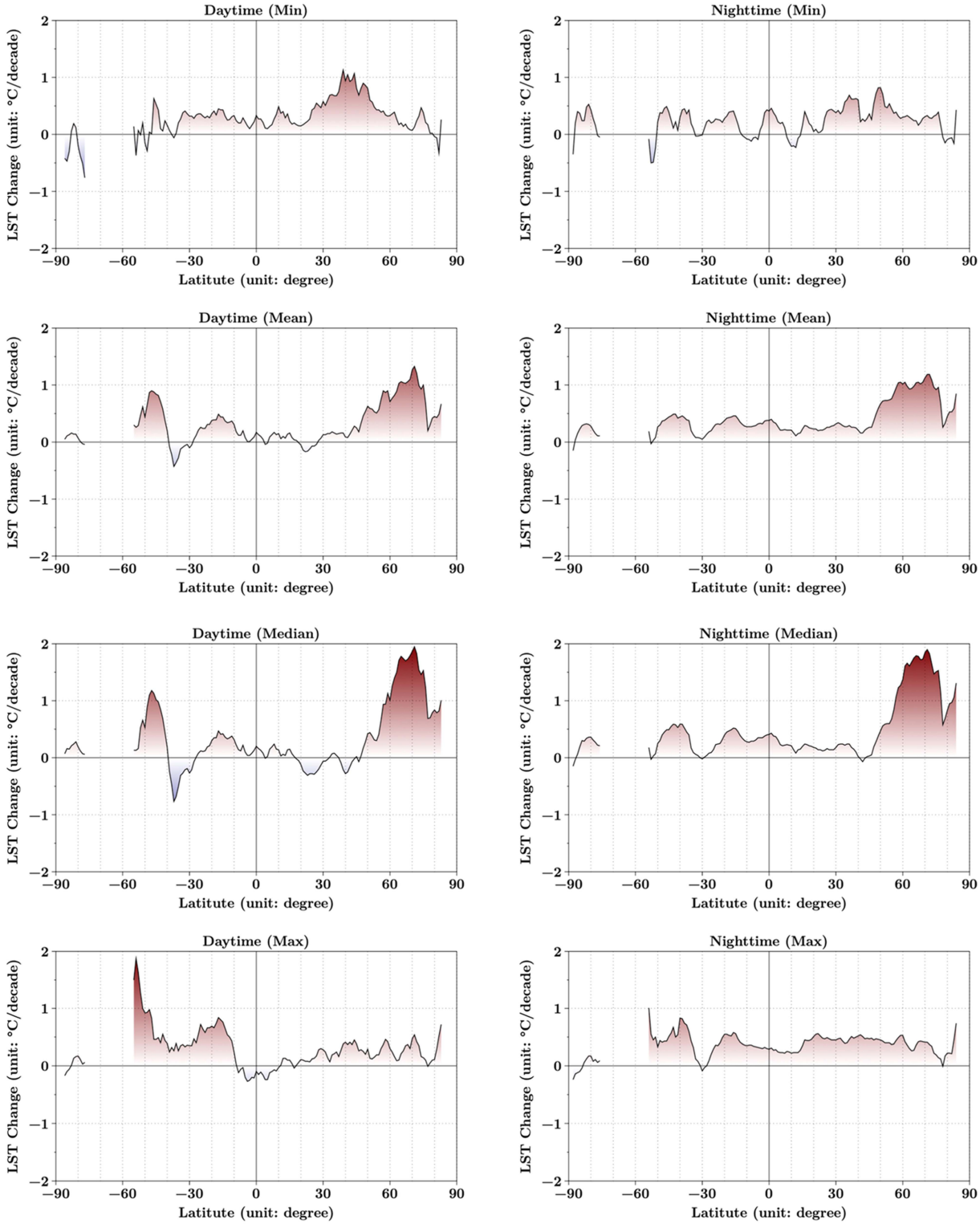

Fig. 4. Longitudinally averaged global LST change rate (°C/decade) from 2003 to 2021. The minimum, mean, median, and maximum LST change for daytime and nighttime are presented in two rows, respectively. Data between the latitude range 84°N–90°N, 55°S–75°S, and 87°S–90°S are absent due to the lack of satellite observations.

warming, in particular, the LST for southern hemisphere Temperate/Cold Zones has been stable or decreasing in the past two decades.

In summary, we found that the LST changes vary significantly for different hemispheres and climate zones. Although both NH and SH experienced increasing LSTs during the study period, there is a significantly more LST increase in the NH than in SH. In addition, the LST changes are not the same in different climate zones. Only one climate zone (SH Cold Zone) experienced a significant LST decrease in daytime minimum LST between

2003 and 2021. Most lower latitude climate zones have not experienced huge LST changes; however, the minimum LSTs for NH Temperate Zone and Subtropics Zone have warmed much faster than other climate zones, with at least 0.68°C/decade for daytime LST and 0.45°C/decade for nighttime LST. The mean and median LST daytime changes in NH Cold Zone are 0.92 and 1.5°C/decade, which are 2.4 times higher than the global mean and 3.2 times higher than the global median, respectively. This result further validated the hypothesis from past research on global climate change that higher latitudes are experiencing most of the global warming, especially for the past few decades [1], [34], [35], [36]. To provide fine spatial variation of global LST changes, we calculated the LST changes by one-degree latitude interval, and the result is shown in Fig. 4.

Although some of the important findings of this research have been discovered in previous research. First, this study provides a quantitative analysis of the latest LST trends for the past decades at 1km spatial resolution, which is valuable for ongoing climate change studies. Although a significant test was not conducted in this experiment, by comparing with IPCC report AR6, the LST changes observed from this study are dramatic [1]. For example, a previous study reported a temperature increase of 1.7°C over a 210-year period [37]. In contrast, our research indicates that urban average temperature can achieve the same increase in less than four decades, as shown in Table III. Figs. 1 and 3 illustrate the frequency of MODIS observations and the rate of LST change across various locations. It is reasonable to infer that locations with substantial LST changes and a greater number of satellite observations exhibit higher reliability. In addition, Table III highlights the LST temporal variation in urban extents, and the result clearly demonstrates that the mean LST increasing speed in the urban areas is faster than the global average. This is potentially contributed by urban expansion and the heat island effect. In addition, a huge difference in increasing speed can be identified for the minimum and maximum LST changes, potentially indicating that warmer winters and extreme summer heat can occur more frequently in human habitats.

C. Limitations and Recommendations

This study has several limitations. First, while the method we employed is general and not tied to specific locations, our conclusions about LST changes and temperature increase rates across different regions and latitudes are based on linear regression. This approach is rough and only suitable for long-term climate trend analysis; however, it cannot accurately capture the dynamics of seasonal temperature changes. Second, the delineation of climate zones is latitude-dependent, and the estimation of urban extent is a rudimentary approximation that might not adequately reflect changes in all metropolitan regions. For instance, two metropolitans located at the same latitude may belong to different climate zones. Furthermore, it is important to note that there is currently no high-resolution urban extent data available that accurately track annual changes in extent at the global level. This limitation can introduce inaccuracies, as the pace of urbanization, urban characteristics, and landscape features vary significantly among different urban areas, and the impacts of global warming are highly location-specific.

In future research, we can improve the spatial accuracy of LST by using 250-m MODIS data, which will demand a substantially increased computational resource allocation. Furthermore, to bolster the precision of our LST change estimations, we can compare the linear regression model with other advanced methods. In addition, we aim to assess LST changes using high spatio-temporal resolution urban extent datasets, particularly within specific urban areas situated in diverse climate zones and characterized by varying socioeconomic conditions. This will empower us to delve into the impact of LST changes on human habitats over the past few decades with unprecedented detail. The result will offer invaluable insights for guiding future urban planning and decision-making, along with actionable recommendations.

IV. Conclusion

This study solved a few difficulties that have not been addressed before. First of all, relying on a powerful online geospatial processing service, the study is able to establish regression models at the pixel level for the entire land surface. Because the method we developed is general and location-independent, it provides the pixel-level models for the global LST change, and the results can delineate the entire dynamics of the LST change for the past 19 years. Second, the study uses both Terra and Aqua satellites to boost the observation frequencies. Using both satellites can improve the model accuracy by having two observation windows in both daytime and nighttime and reducing outliers. Third, we calculated the trends of minimum, mean, median, and maximum MODIS LST trends for providing evaluations from different angles while most other studies only focus on mean LST. More importantly, the LST change dataset can be easily utilized in different applications such as cropland change analysis, and potential cropland identification due to climate change. Future studies are needed to fully understand the relationship between LST trends and extreme weather, especially for human habitats. Our LST change maps can serve as important datasets for high-resolution global climate change studies in the future. The proposed GEE-based pixel-level regression model can be potentially transferred to different temporal ranges or similar satellite sensors with little effort. The findings of this study can help us to better understand LST change for the entire Earth's land surface in the 21st century.

Acknowledgment

Data and Code Availability: The Global LST change (2003–2021) data are available for download from the Zenodo repository at https://doi.org/10.5281/zenodo.6991410. LST change layers are stored in .tif format, and other files in the folder store supportive information about the data. For example, georeferencing information is stored in the .tfw file. The folder is compressed and stored in.zip format to reduce the file size. The data can be viewed using various GIS software such as ESRI ArcGIS Pro (https://www.esri.com/) and QGIS (https://qgis.org/).

The scripts used to generate the Global LST change dataset and MODIS mask layers are available in this GitHub repository: https://github.com/llin-csiss/GLobal-LST-Change

REFERENCES

[1] B. Bednar-Friedl, R. Biesbroek, and D. N. Schmidt, "IPCC Sixth Assessment Report (AR6): Climate change 2022 - Impacts, adaptation and vulnerability: Regional factsheet Europe," 2022. [Online]. Available: https://policycommons.net/artifacts/2264317/ipcc_ar6_wgii_factsheet_europe/3023371/, Accessed: Jul. 17, 2022.

[2] A. Sekertekin and S. Bonafoni, "Land surface temperature retrieval from Landsat 5, 7, and 8 over rural areas: Assessment of different retrieval algorithms and emissivity models and toolbox implementation," *Remote Sens.*, vol. 12, no. 2, Jan. 2020, Art. no. 294, doi: 10.3390/rs12020294.

[3] J. A. Sobrino, J. C. Jiménez-Muñoz, and L. Paolini, "Land surface temperature retrieval from Landsat TM 5," *Remote Sens. Environ.*, vol. 90, no. 4, pp. 434–440, Apr. 2004, doi: 10.1016/j.rse.2004.02.003.

[4] Y. Yan et al., "Driving forces of land surface temperature anomalous changes in North America in 2002–2018," *Sci. Rep.*, vol. 10, no. 1, Dec. 2020, Art. no. 6931, doi: 10.1038/s41598-020-63701-5.

[5] J. Hansen, R. Ruedy, M. Sato, and K. Lo, "Global surface temperature change," *Rev. Geophys.*, vol. 48, no. 4, 2010, Art. no. RG4004, doi: 10.1029/2010RG000345.

[6] S. Rahmstorf and D. Coumou, "Increase of extreme events in a warming world," *Proc. Nat. Acad. Sci. USA*, vol. 108, no. 44, pp. 17905–17909, Nov. 2011, doi: 10.1073/pnas.1101766108.

[7] Y. Fan and H. van den Dool, "A global monthly land surface air temperature analysis for 1948–present," *J. Geophys. Res., Atmos.*, vol. 113, no. D1, 2008, Art. no. D01103, doi: 10.1029/2007JD008470.

[8] J. Hansen, M. Sato, R. Ruedy, K. Lo, D. W. Lea, and M. Medina-Elizade, "Global temperature change," *Proc. Nat. Acad. Sci. USA*, vol. 103, no. 39, pp. 14288–14293, Sep. 2006, doi: 10.1073/pnas.0606291103.

[9] N. A. Rayner et al., "Global analyses of sea surface temperature, sea ice, and night marine air temperature since the late nineteenth century," *J. Geophys. Res., Atmos.*, vol. 108, no. D14, 2003, Art. no. 4407, doi: 10.1029/2002JD002670.

[10] Z.-L. Li et al., "Satellite-derived land surface temperature: Current status and perspectives," *Remote Sens. Environ.*, vol. 131, pp. 14–37, Apr. 2013, doi: 10.1016/j.rse.2012.12.008.

[11] T. Liu, L. Yu, and S. Zhang, "Land surface temperature response to irrigated paddy field expansion: A case study of semi-arid western Jilin Province, China," *Sci. Rep.*, vol. 9, no. 1, Mar. 2019, Art. no. 5278, doi: 10.1038/s41598-019-41745-6.

[12] T. M. Smith, R. W. Reynolds, T. C. Peterson, and J. Lawrimore, "Improvements to NOAA's historical merged land–ocean surface temperature analysis (1880–2006)," *J. Clim.*, vol. 21, no. 10, pp. 2283–2296, May 2008, doi: 10.1175/2007JCLI2100.1.

[13] L. Zhou, Y. Tian, S. B. Roy, C. Thorncroft, L. F. Bosart, and Y. Hu, "Impacts of wind farms on land surface temperature," *Nature Clim. Change*, vol. 2, no. 7, pp. 539–543, Jul. 2012, doi: 10.1038/nclimate1505.

[14] S.-B. Duan et al., "Land surface temperature retrieval from passive microwave satellite observations: State-of-the-art and future directions," *Remote Sens.*, vol. 12, no. 16, Jan. 2020, Art. no. 2573, doi: 10.3390/rs12162573.

[15] W. Zhao, M. Yang, R. Chang, Q. Zhan, and Z. Li, "Surface warming trend analysis based on MODIS/Terra land surface temperature product at Gongga Mountain in the southeastern Tibetan Plateau," *J. Geophys. Res., Atmos.*, vol. 126, no. 22, Nov. 2021, Art. no. e2020JD034205, doi: 10.1029/2020JD034205.

[16] J. Muro et al., "Land surface temperature trends as indicator of land use changes in wetlands," *Int. J. Appl. Earth Observ. Geoinf.*, vol. 70, pp. 62–71, Aug. 2018, doi: 10.1016/j.jag.2018.02.002.

[17] S.-B. Duan et al., "Validation of collection 6 MODIS land surface temperature product using in situ measurements," *Remote Sens. Environ.*, vol. 225, pp. 16–29, May 2019, doi: 10.1016/j.rse.2019.02.020.

[18] A. Jia, H. Ma, S. Liang, and D. Wang, "Cloudy-sky land surface temperature from VIIRS and MODIS satellite data using a surface energy balance-based method," *Remote Sens. Environ.*, vol. 263, Sep. 2021, Art. no. 112566, doi: 10.1016/j.rse.2021.112566.

[19] J. Liu, D. F. T. Hagan, and Y. Liu, "Global land surface temperature change (2003–2017) and its relationship with climate drivers: AIRS, MODIS, and ERA5-land based analysis," *Remote Sens.*, vol. 13, no. 1, , Jan. 2021, Art. no. 44, doi: 10.3390/rs13010044.

[20] K. B. Mao et al., "Global surface temperature change analysis based on MODIS data in recent twelve years," *Adv. Space Res.*, vol. 59, no. 2, pp. 503–512, Jan. 2017, doi: 10.1016/j.asr.2016.11.007.

[21] W. Zhu, A. Lű, and S. Jia, "Estimation of daily maximum and minimum air temperature using MODIS land surface temperature products," *Remote Sens. Environ.*, vol. 130, pp. 62–73, Mar. 2013, doi: 10.1016/j.rse.2012.10.034.

[22] H. Ebrahimy, H. Aghighi, M. Azadbakht, M. Amani, S. Mahdavi, and A. A. Matkan, "Downscaling MODIS land surface temperature product using an adaptive random forest regression method and Google Earth Engine for a 19-years spatiotemporal trend analysis over Iran," *IEEE J. Sel. Topics Appl. Earth Observ. Remote Sens.*, vol. 14, pp. 2103–2112, 2021, doi: 10.1109/JSTARS.2021.3051422.

[23] S. L. Ermida, P. Soares, V. Mantas, F.-M. Göttsche, and I. F. Trigo, "Google Earth Engine open-source code for land surface temperature estimation from the Landsat series," *Remote Sens.*, vol. 12, no. 9, Jan. 2020, Art. no. 1471, doi: 10.3390/rs12091471.

[24] N. Gorelick, M. Hancher, M. Dixon, S. Ilyushchenko, D. Thau, and R. Moore, "Google Earth Engine: Planetary-scale geospatial analysis for everyone," *Remote Sens. Environ.*, vol. 202, pp. 18–27, Dec. 2017, doi: 10.1016/j.rse.2017.06.031.

[25] Z. Wan, "New refinements and validation of the MODIS land-surface temperature/emissivity products," *Remote Sens. Environ.*, vol. 112, no. 1, pp. 59–74, Jan. 2008, doi: 10.1016/j.rse.2006.06.026.

[26] O. Mutanga and L. Kumar, "Google Earth Engine applications," *Remote Sens.*, vol. 11, no. 5, Jan. 2019, Art. no. 591, doi: 10.3390/rs11050591.

[27] A. Savtchenko et al., "Terra and Aqua MODIS products available from NASA GES DAAC," *Adv. Space Res.*, vol. 34, no. 4, pp. 710–714, Jan. 2004, doi: 10.1016/j.asr.2004.03.012.

[28] C. Vancutsem, P. Ceccato, T. Dinku, and S. J. Connor, "Evaluation of MODIS land surface temperature data to estimate air temperature in different ecosystems over Africa," *Remote Sens. Environ.*, vol. 114, no. 2, pp. 449–465, Feb. 2010, doi: 10.1016/j.rse.2009.10.002.

[29] W. Wang, S. Liang, and T. Meyers, "Validating MODIS land surface temperature products using long-term nighttime ground measurements," *Remote Sens. Environ.*, vol. 112, no. 3, pp. 623–635, Mar. 2008, doi: 10.1016/j.rse.2007.05.024.

[30] M. Zhao, C. Cheng, Y. Zhou, X. Li, S. Shen, and C. Song, "A global dataset of annual urban extents (1992–2020) from harmonized nighttime lights," *Earth Syst. Sci. Data*, vol. 14, pp. 517–534, 2022, doi: 10.5194/essd-2021-302.

[31] Z. Wan, "Collection-5 MODIS land surface temperature products users' guide," Inst. Comput. Earth Sys. Sci., Univ. California Santa Barbara, Santa Barbara, CA, USA, 2007.

[32] L. Guo, L. Di, C. Zhang, L. Lin, F. Chen, and A. Molla, "Evaluating contributions of urbanization and global climate change to urban land surface temperature change: A case study in Lagos, Nigeria," *Sci. Rep.*, vol. 12, no. 1, Aug. 2022, Art. no. 14168, doi: 10.1038/s41598-022-18193-w.

[33] D. Cui, S. Liang, and D. Wang, "Observed and projected changes in global climate zones based on Köppen climate classification," *WIREs Clim. Change*, vol. 12, no. 3, 2021, Art. no. e701, doi: 10.1002/wcc.701.

[34] T. L. Delworth and T. R. Knutson, "Simulation of early 20th century global warming," *Science*, vol. 287, no. 5461, pp. 2246–2250, Mar. 2000, doi: 10.1126/science.287.5461.2246.

[35] R. A. Kerr, "Global warming is changing the world," *Science*, vol. 316, no. 5822, pp. 188–190, Apr. 2007, doi: 10.1126/science.316.5822.188.

[36] W.-Y. Wu, C.-W. Lan, M.-H. Lo, J. T. Reager, and J. S. Famiglietti, "Increases in the annual range of soil water storage at northern middle and high latitudes under global warming," *Geophys. Res. Lett.*, vol. 42, no. 10, pp. 3903–3910, 2015, doi: 10.1002/2015GL064110.

[37] N. Morueta-Holme, K. Engemann, P. Sandoval-Acuña, J. D. Jonas, R. M. Segnitz, and J.-C. Svenning, "Strong upslope shifts in Chimborazo's vegetation over two centuries since Humboldt," *Proc. Nat. Acad. Sci. USA*, vol. 112, no. 41, pp. 12741–12745, Oct. 2015, doi: 10.1073/pnas.1509938112.

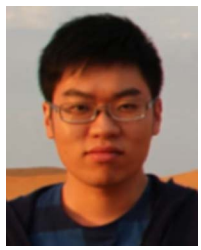

Li Lin (Member, IEEE) received the Ph.D. degree in Earth systems and geoinformation sciences from George Mason University, Fairfax, VA, USA, in 2022.

He is currently a Research Assistant Professor with the Center for Spatial Information Science and Systems, George Mason University. He has authored or coauthored more than 50 peer-reviewed journal articles, book chapters, conference papers, and engineering reports. He leads the development of many geospatial data service systems to serve the geosciences and remote sensing community. His research interests include agro-geoinformatics, remote sensing, urban development, geospatial metadata, and catalog federation.

Liping Di (Senior Member, IEEE) received the Ph.D. degree in remote sensing/GIS (geography) from the University of Nebraska–Lincoln, Lincoln, NE, USA, in 1991.

He is currently a Professor and the Founding Director of the Center for Spatial Information Science and Systems and a Professor with the Department of Geography and Geoinformation Science, George Mason University, Fairfax, VA, USA. He has engaged in geoinformatics and remote sensing research for more than 30 years. He has authored or coauthored more than 550 publications.

Dr. Di actively participated in the activities of several professional societies and international organizations, such as IEEE GRSS, ISPRS, CEOS, ISO Technical Committee 211 (ISO TC 211), OGC, INCITS, and GEO. He chaired INCITS/L1, a U.S. National Committee responsible for setting U.S. National standards on geographic information and representing the U.S. at ISO TC 211 from 2010 to 2016 and was the Convenor of ISO TC 211 Working Group 9 from 2019 to 2022. He was elected as the inaugural President of the International Society of Agromatics in 2022. He was the Co-Chair of the Data Archiving and Distribution Technical Committee (DAD TC) of IEEE GRSS from 2002 to 2005 and the Chair of DAD TC from 2005 to 2009. He was one of the founders of the Earth Science Informatics Technical Committee of IEEE GRSS. In 2012, he founded the Annual International Conference on Agro-Geoinformatics, an IEEE GRSS-sponsored specialty conference, and has served as the general conference Chair since then. He is the General Chair of IGARSS 2026. He was a recipient of many prestigious awards for his work, such as the Merit Award in 2016 and the Lifetime Achievement Award from the International Committee for Information Technology Standards in 2022. He is the recipient of research grants of more than $64 million.

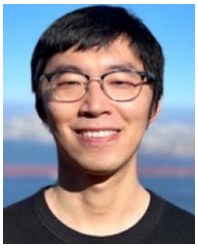

Chen Zhang (Member, IEEE) received the Ph.D. degree in earth systems and geoinformation sciences from George Mason University, Fairfax, VA, USA, in 2021.

He is currently a Research Assistant Professor with the Center for Spatial Information Science and Systems, George Mason University, Fairfax, VA, USA. He has authored or coauthored more than 50 peer-reviewed journal articles, book chapters, conference papers, and engineering reports. He leads the development of many geospatial data service systems to serve the geosciences and remote sensing community. His research interests include geographic information science and systems, remote sensing, agro-geoinformatics, geospatial information interoperability and standards, and land use and land cover change.

Liying Guo (Member, IEEE) received the Doctor of Science degree in cartography and geographic information systems from Shaanxi Normal University, Xi'an, China, in 2008.

She is currently a Research Professor and an Associate Director with the Center for Spatial Information Science and Systems, George Mason University, Fairfax, VA, USA. She has engaged in geospatial information research for more than 25 years. Her research interests include geospatial science applications, food security, ecosystem sustainability, public health, climate change, and land use and land cover change. She has actively participated in the activities of IEEE GRSS, ISO TC211, INCITS, and OGC, and was a PI and Co-PI on multiple federal and national research grants.

Dr. Guo is a Secretary of the International Society of Agromatics, the Co-Chair of the Organizing Committee of the Annual International Conference on Agro-Geoinfomatics, and the Coordinator of the NSF-funded multi-institutional and multidisciplinary WaterSmart project. She is also a member of the scientific committee, academic editorial board, and organizing committee on multiple international conferences and workshops.